ANNALI DI GEOFISICA, VOL. XXXIX, N. 1, January 1996

Effects of resistive bodies on DC electrical soundings

Mauro Giudici and Luigi Alfano
Dipartimento di Scienze della Terra, Sezione di Geofisica, Università di Milano, Italy

Abstract
Some deep DC electrical soundings, performed in alpine and apenninic areas with the continuous polar dipole-dipole spread, show apparent resistivity curves with positive slopes. Measured values of apparent resistivity reach 30000 Ωm. Applying the «surface charges» method we developed three dimensional mathematical models, by means of which we can state simple rules for determining the minimum extensions of the deep resistive bodies, fundamental information for a more precise interpretation of the field results.

Key words *DC electrical sounding – dipole-dipole spread – 3-D mathematical modelling*

1. Introduction

The dipole-dipole system is very useful to execute deep DC electrical soundings (Alfano, 1974, 1980). In fact, it allows great exploration depths to be reached without unrolling very long cables, as is the case for Schlumberger spreads. This has a number of advantages, both with respect to field operations and because the possible effects of leakage from the cable far from the energising electrodes are limited.

The continuous polar dipole-dipole method consists in realising an array whose scheme is drawn in fig. 1a. The potentiometric dipole MN, whose centre is the point O, is kept fixed and the current dipoles (A and B) are moved far away so that the direction of MN coincides with the direction of AB (polar array) and the position of the farthest electrode of a dipole is the same as that of the nearest electrode of the following dipole (continuous array).

The measurements obtained with a continuous polar dipole-dipole spread are very much affected by lateral variations, which introduce many problems in the interpretation stage. However, with a mathematical operation we can convert the results of a continuous polar dipole-dipole array to those which would have been obtained with a half-Schlumberger spread (Al'pin, 1950, 1958; Patella, 1974), for which MN is in the same position as for the double-dipole array whereas the current poles are coincident with the current electrodes of the double-dipole array (see fig. 1b). The half-Schlumberger diagram is smoother, less affected by horizontal inhomogeneities and, as a consequence, more useful for the interpretation in terms of depth. However, it has been shown that the transformation from a general dipole-dipole diagram to the half-Schlumberger one is valid only if the subsurface has a plane parallel layering; in real cases the geological structures are three-dimensional and the polar array is the only one for which the transformation is applicable (Alfano, 1980, 1993).

For a thorough and comprehensive description of the transformation procedure we refer the reader to already published papers (Alfano, 1974, 1980, 1993).

In recent years several DC electrical soundings with the continuous polar dipole-dipole

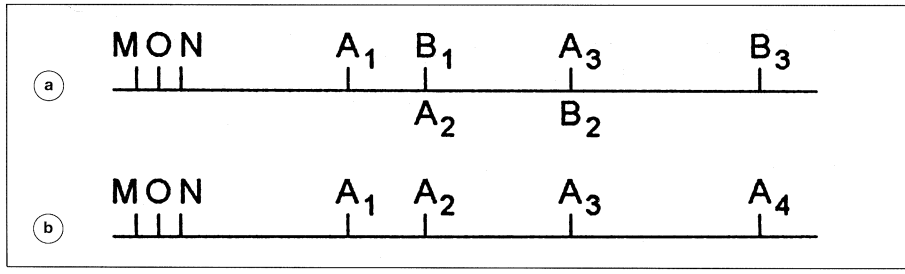

Fig. 1a,b. a) Continuous polar dipole-dipole spread: O - centre of the potentiometric dipole; MN - potentiometric dipole; A_1B_1, A_2B_2, ... - current dipoles. b) Half-Schlumberger spread: O - centre of the potentiometric dipole; MN - potentiometric dipole; A_1, A_2, ... - current poles.

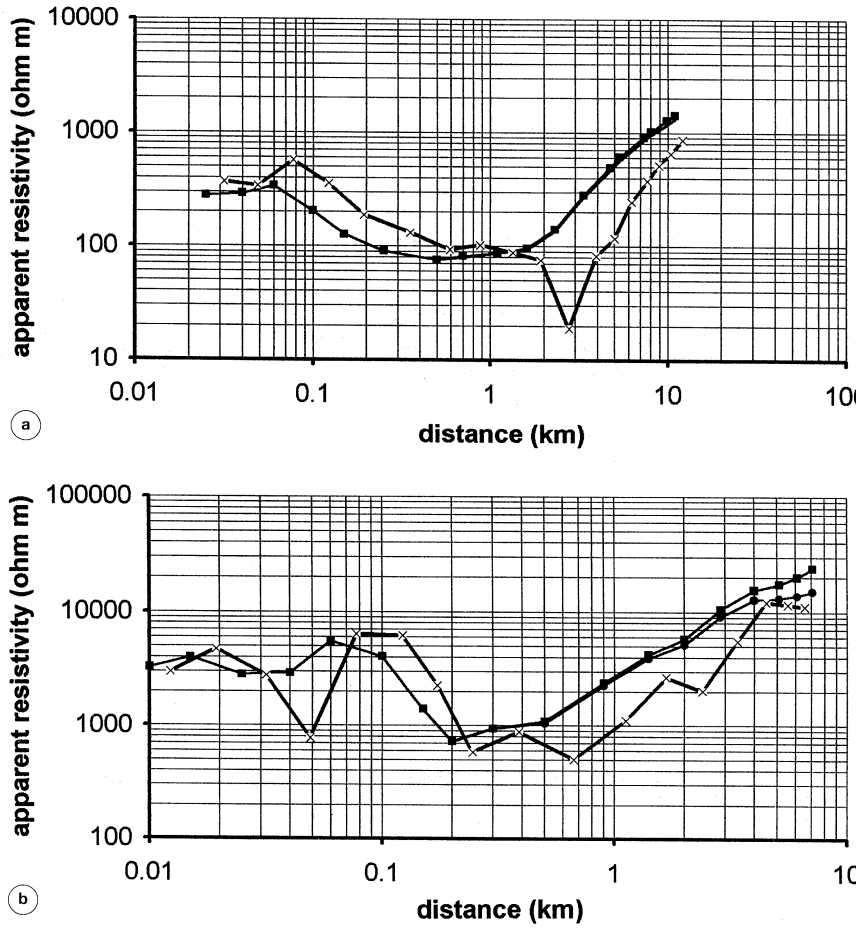

Fig. 2a,b. Examples of apparent resistivity curves obtained in Northern Apennines (a) and Central Alps (b). ×: dipole-dipole curve; ■ ●: transformed half-Schlumberger curves.

method have been carried out both in the Central Alps and Northern Apennines. The greatest distance between the dipoles has been about 20 km, which corresponds to an exploration depth of about 7 km in the most favourable cases. In this work we consider some soundings whose apparent resistivity diagrams have strong positive slopes (fig. 2a,b) indicating the existence of resistive beds.

The interpretation of these soundings requires not only the determination of the minimum thickness of these resistive bodies but also their minimum lateral extension. This last datum is very important, because it can lead to a better geophysical interpretation of the soundings with three-dimensional structures.

For this purpose we developed mathematical models for computing half-Schlumberger curves for a resistive body lying at some depth and with limited lateral extension. With these models we obtained useful information for the interpretation of field diagrams such as those in fig. 2a,b.

2. The «surface charges» method

A mathematical model for computing theoretical apparent resistivity curves requires the solution of the equation

$$\text{div } \vec{j} = 0, \text{ with } \vec{j} = \vec{E}/\rho, \qquad (2.1)$$

where $\vec{j}$ is the electrical charge flow density, $\vec{E}$ is the electrical field and ρ is the electrical resistivity. Equation (2.1) must be accompanied by appropriate boundary conditions, which we describe making reference to fig. 3. Let us consider the Earth as a half-space limited by the plane corresponding to the ground surface (S_0). Below the plane ground surface there are geological bodies with different values of electrical resistivity. Let us suppose a current I is injected into the Earth through a current electrode at the point Q: S_1 denotes the surface of the electrode. The boundary conditions are the following:

i) null flux in the direction perpendicular to S_0;

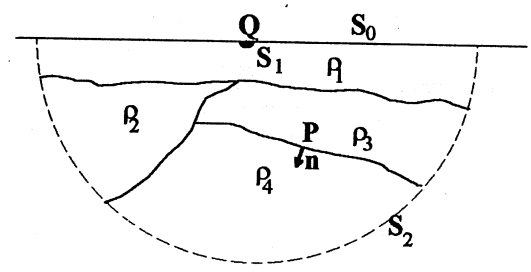

Fig. 3. S_0: Earth surface; S_1: surface of the current electrode; S_2: surface at infinity.

ii) known flux for S_1;

iii) null potential for S_2. In fact S_2 is a surface at the infinity and for this reason it has been drawn as a dashed line in fig. 3.

The numerical solution to eq. (2.1) with the above mentioned boundary conditions can be obtained with several methods. Among others we recall the finite difference, the finite element and the surface charge methods.

Finite differences are not very efficient to discretise three-dimensional domains when the surfaces of discontinuity of electrical resistivity are very complicated. The finite element method is more efficient for this problem, but there are still problems for the approximation of the surface at infinity, S_2. Moreover for both these methods the number of unknowns is usually extremely great.

The «surface charge» method (Alfano, 1959, 1984), also known as «integral equation method» (Dieter *et al.*, 1969) or «boundary element method» (Okabe, 1981), is to be preferred for simulating the response of bodies limited by closed surfaces. This is the method that we use. The solution to eq. (2.1) is obtained by separating the electrical field into two terms: the primary field, $\vec{E}_p$, due to the current electrode and corresponding to the field in a homogeneous medium with $\rho = \rho_1$, and the secondary field, $\vec{E}_s$, which is different from zero if discontinuities of electrical resistivity in the subsurface exist. The secondary field is computed by supposing that electrical charges – induced by the electrical field – are present on the discontinuity surfaces. If Σ denotes the

set of all the discontinuity surfaces and $\sigma(P)$ is the surface charge density at the point $P \in \Sigma$, $\sigma(P)$ must satisfy the equation

$$\frac{2\pi}{K(P)}\sigma(P) = \tag{2.2}$$

$$= \Gamma(P, Q)\frac{\rho_1 I}{2\pi} + \int_{\Sigma'} \Gamma(P, P')\,\sigma(P')\,dS(P'),$$

where:

i) $K(P)$ is the «reflection coefficient», given by $K(P) = (\rho(P_+) - \rho(P_-))/(\rho(P_+) + \rho(P_-))$, $\rho(P_+)$ and $\rho(P_-)$ being the values of electrical resistivity on the two sides of the discontinuity close to the point P;

ii) $\Sigma' = \Sigma - d\Sigma(P)$, $d\Sigma(P)$ being an infinitesimal area centred at the point P;

iii) $\Gamma(P,P') = \vec{P'P} \cdot \vec{n}(P)/|\vec{P'P}|^3$ and analogously $\Gamma(P,Q)$, $\vec{n}(P)$ being the normal to Σ at the point P.

The first term in the right hand side of eq. (2.2) represents the normal component of the primary field, $\vec{E}_p(P) \cdot \vec{n}(P)$, whereas the second one is the normal component of the secondary field, $\vec{E}_s(P) \cdot \vec{n}(P)$. Equation (2.2) is derived from the continuity conditions for the tangential component of $\vec{E}$ and the normal component of $\vec{j}$ across a surface of discontinuity for ρ (Alfano, 1959, 1984, 1993).

Generally the surface Σ also includes the Earth surface, when S_0 is not plane. Since we suppose the ground surface S_0 to be plane, we can avoid considering the surface charge density on the Earth surface introducing the images of the underground discontinuity surfaces with respect to S_0. The surface charge density distributed over an image area is equal to the charge distributed on the original area. In such a way the null flux boundary condition on S_0 is strictly verified. From now on, we consider Σ as the set of the discontinuity surfaces below the topographic surface and of their images with respect to S_0.

The potential and the electrostatic field at an arbitrary point P are given by

$$V(P) = \frac{\rho_1 I}{2\pi}\frac{1}{|\vec{QP}|} + \int_\Sigma \frac{1}{|\vec{P'P}|}\sigma(P')\,dS(P'), \tag{2.3}$$

$$\vec{E}(P) = \frac{\rho_1 I}{2\pi}\frac{\vec{QP}}{|\vec{QP}|^3} + \int_\Sigma \frac{\vec{P'P}}{|\vec{P'P}|^3}\sigma(P')\,dS(P').$$

In conclusion, the resolution of equation (2.1) requires, first of all, that the surface charge distribution, $\sigma(P)$, solution of eq. (2.2) be determined. Subsequently the potential and the electrical field are computed with eq. (2.3).

The integral eq. (2.2) can be solved numerically. Let us consider the discontinuity surfaces as a collection of N small plane areas: P_j, $\vec{n}_j$ and S_j denote, respectively, the barycentre, the normal versor and the surface of the j-th area. The indices i and j vary from 1 to N. Let us substitute the surface charge density, which is actually continuously distributed over every area, with a point charge concentrated in the barycentre of the area. The value of the total charge for the i-th area is denoted by $\sigma_i S_i$. Under these hypotheses, eq. (2.2) becomes

$$\frac{2\pi}{K_i}\sigma_i = \Gamma(P_i, Q)\frac{\rho_1 I}{2\pi} + \sum_{j \neq i} \Gamma(P_i, P_j)\,\sigma_j S_j, \tag{2.4}$$

which is a system of linear equations. The solution to this linear system can be obtained with an iterative procedure. We start with a tentative solution, $\sigma_i^{(0)}$, and we compute the values of the charges at the $(n+1)$-th iteration by the recursive formula:

$$\sigma_i^{(n+1)} = \frac{K_i}{2\pi}\left\{\Gamma(P_i, Q)\frac{\rho_1 I}{2\pi} + \sum_{j \neq i} \Gamma(P_i, P_j)\,\sigma_j^{(n)} S_j\right\}. \tag{2.5}$$

It has been proved that this iterative algorithm converges (Alfano, 1959). The conver-

gence velocity can be increased by means of the Gauss-Seidel method (Young, 1971), which uses all the already updated values of $\sigma_j^{(n+1)}$ instead of $\sigma_j^{(n)}$ at every stage of the computation of $\sigma_i^{(n+1)}$ with eq. (2.5). Having solved the system (2.4), we compute the electrical field at every point of the domain with

$$\vec{E}(P) = \frac{\rho_1 I}{2\pi} \frac{\vec{QP}}{|\vec{QP}|^3} + \sum_i \frac{\vec{P_iP}}{|\vec{P_iP}|^3} \sigma_i S_i, \qquad (2.6)$$

which is a simple discretisation of the second eq. of (2.3).

The computer code for the solution to the linear system (2.4) and the computation of apparent resistivities has been written in the C programming language to take advantage of the memory and velocity of modern PCs. In particular, the code run on a PC with a 486DX/50 processor and 16MB RAM. The computation of an apparent resistivity curve for the most complex cases (with $N \approx 1700$) required about 1000 s of CPU time.

3. Numerical results

In this work we consider a simple model for the resistive body – a parallelepiped – with the geometry shown in fig. 4. The top of the parallelepiped is parallel to the ground plane and lies at a depth h below the topographic surface. The thickness of the parallelepiped is 10 times h, whereas its extensions along the x and y directions are denoted respectively by Δx and Δy. The sounding direction is along the positive x-axis. The potentiometric dipole MN is located at the origin of the Cartesian axes for the cases shown in figs. 5a-c and 6, at a distance 5 h from the projection on the surface of the border of the parallelepiped. Instead, the results of fig. 7a-c refer to the potentiometric dipole located at M′N′, *i.e.*, 5 h before the above mentioned projection. We considered an electrical resistivity for the resistive body 100 times higher than the resistivity of surrounding rocks: this corresponds to a «reflection coefficient» $K = 0.980198$.

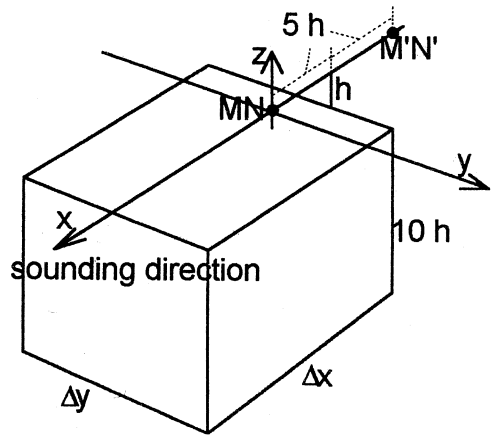

Fig. 4. Geometry of the model used for the numerical simulations.

The apparent resistivity curves for a half-Schlumberger array are computed for different values of the dimensions of the parallelepiped both in the longitudinal (Δx) and in the transversal (Δy) directions with respect to the spread direction. Our purpose is to evaluate the effects of the vertical boundaries of the body, in order to find out simple rules to determine the minimum extensions of resistive bodies, whose existence is evident from field diagrams. Therefore we consider as a reference the apparent resistivity curve computed for the case of three plane parallel layers, with geometrical and electrical characteristics analogous to those of the model in fig. 4. In particular, we have the first layer with a thickness h and $\rho = \rho_1$; the second layer with a thickness 10 h and $\rho = 100\ \rho_1$; and finally the semi-infinite bed with $\rho = \rho_1$.

In the following diagrams of apparent resistivity we use adimensional values for lengths and apparent resistivities. In particular, lengths and apparent resistivities should be considered as divided by h and ρ_1, respectively. The results are valid for any geometrically and electrically similar model: the real appropriate values for h and ρ_1 have to be considered.

Figure 5a-c shows the computed diagrams of apparent resistivity, when the potentiometric

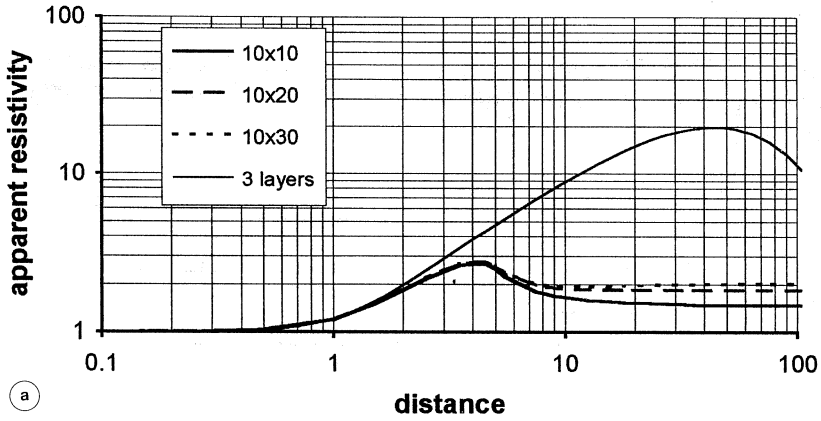

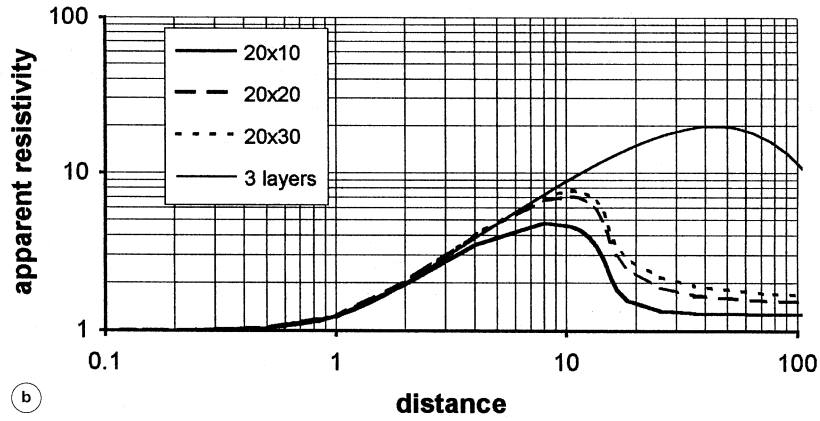

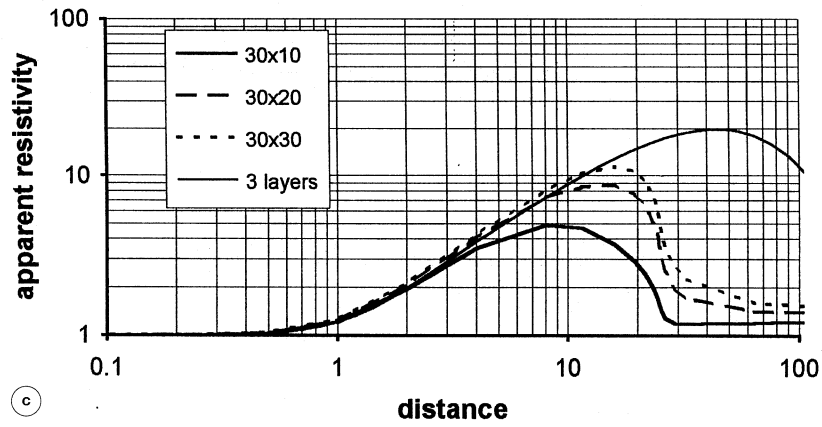

Fig. 5a-c. Apparent resistivity curves: the longitudinal – Δx – and transversal – Δy – extensions of the resistive body are shown in the legend. Apparent resistivities and lengths are adimensional (see text for details).

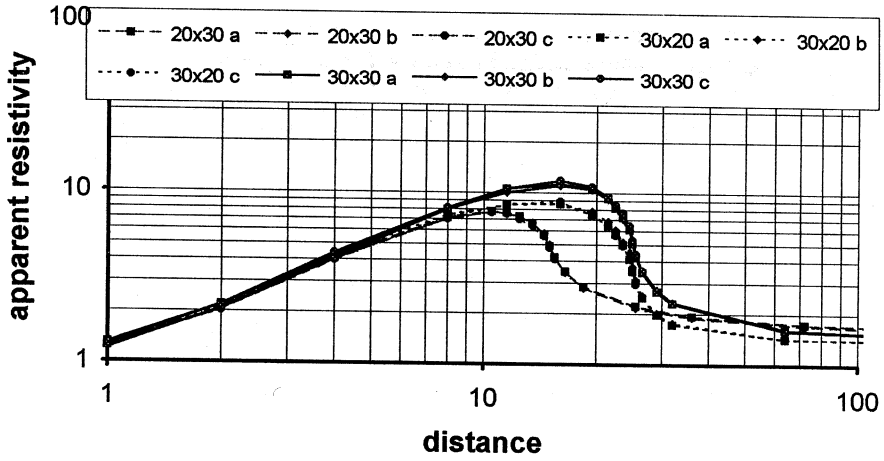

Fig. 6. Comparison among diagrams of apparent resistivities computed with different approximations. Apparent resistivities and lengths are adimensional (see text for details).

dipole is in MN (see fig. 4). In particular, fig. 5a compares the three-layers curve with the curves obtained when $\Delta x = 10\ h$ and Δy varies, *i.e.*, for parallelepipeds with a limited extension along the profile. Figure 5a shows that the curves for the parallelepiped can be distinguished from the three-layers one for distances of about 2 h. Figure 5b refers to $\Delta x = 20\ h$. The curve for the smallest body ($\Delta y = 10\ h$) differs from the three-layers curve at distances of about 3 h, whereas the curves for $\Delta y = 20\ h$ and $\Delta y = 30\ h$ follow the trend of the three-layers curve up to distances of the order of 7 h and 10 h, respectively, *i.e.*, at about 8 h and 15 h from the projection of the border of the parallelepiped on the Earth's surface. Figure 5c corresponds to $\Delta x = 30\ h$. Once again the curve for $\Delta y = 10\ h$ differs from the three-layers case at distances of about 3 h, whereas the other curves are still close to the reference curve up to 7 h and 12 h, respectively.

One of the most important problems is the validity of the approximations introduced to discretise the integral eq. (2.2) by means of eq. (2.4). In this case we control the validity of the obtained solutions checking the consistency of the computing procedure. Above all for the greatest bodies, when approximations are greater, we consider different discretisations, varying the number, the geometrical form and the dimensions of the areas used to discretise the discontinuity surface. The results for some trial experiments are represented in fig. 6. Every curve of apparent resistivity actually consists of three curves. The superposition of the computed values is so good that the three curves cannot be easily distinguished. We believe that this check of the algorithm and of the computer code shows that the results are confident and not affected by discretisation errors.

Figure 5a-c shows the sharp variation of apparent resistivity when the border of the parallelepiped is crossed. This variation cannot be reproduced by any theoretical diagram related to a pure plane-parallel layering with infinite lateral extension. This is even more evident in fig. 7a-c, which shows the results when the potentiometric dipole is displaced 5 h before the border of the parallelepiped at the position denoted by M′N′ in fig. 4. We clearly observe the sharp variations of apparent resistivity corresponding to discontinuities which are perpendicular to the profile. The effect of the discontinuities elongated in a direction parallel to the profile is less evident and similar to the variations induced by horizontal layering.

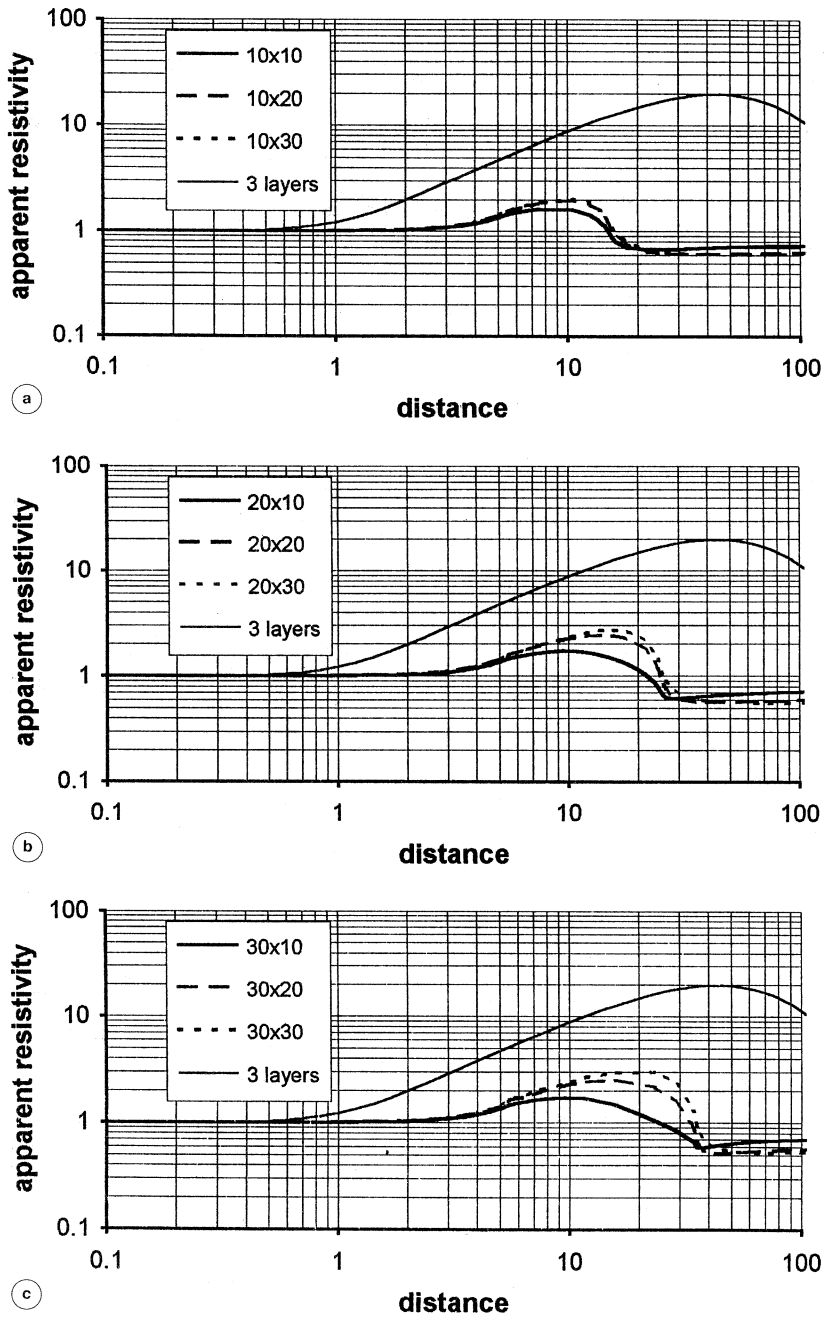

Fig. 7a-c. Apparent resistivity curves for the potentiometric dipole at M′N′ (see fig. 4): the longitudinal – Δx – and transversal – Δy – extensions of the body are shown in the legend. Apparent resistivities and lengths are adimensional (see text for details).

4. Conclusions

The numerical results presented in this paper have an important effect upon the interpretation of field measurements. In fact, if we go back to the examples of field diagrams shown in fig. 2, which put in evidence the existence of resistive beds, we can introduce simple rules for determining the minimum areal extension of such resistive bodies.

In particular, if the top of the resistive bed is at a depth h = 1 km and if the diagrams of apparent resistivity for half-Schlumberger spread show a positive slope for distances up to 10 km, we can state that the resistive body causing this effect is extended for at least 5 km along the profile and for at least 20 km in the transversal direction. If the positive slope is evident for distances greater than 15 km, we conclude that the resistive body extends for more than 10 and 30 km, respectively, longitudinally and transversally to the profile.

These results were obtained for particular dimensions of the anomalous body, but they can be extended to geometrically and electrically similar cases.

As a confirmation of known results, it is also evident from our models that the effect of a discontinuity which intersects the profile is very different from the effect of discontinuities which are elongated in the same direction as the profile. Namely, apparent resistivity shows sharp variations where the profile intersects the projection of the discontinuities on the surface (fig. 7a-c): these variations are even more evident in a dipole sounding.

Acknowledgements

This paper is based on the presentation given at the «V Workshop di Geoelettromagnetismo» (Martina Franca (TA) - Italy - 15-17 September 1993) and was funded by MURST 40%.

REFERENCES

ALFANO, L. (1959): Introduction to the interpretation of resistivity measurements for complicated structural conditions, *Geophys. Prospect.*, **7**, 311-366.

ALFANO, L. (1974): A modified geoelectrical procedure using polar-dipole arrays. An example of application to deep exploration, *Geophys. Prospect.*, **22**, 510-525.

ALFANO, L. (1980): Dipole-dipole deep geoelectrical soundings over geological structures, *Geophys. Prospect.*, **28**, 283-296.

ALFANO, L. (1984): A computation method for DC geoelectric fields over complicated structures, in *Geophysics and Geothermal Areas: State of the Art and Future Developments*, edited by A. RAPOLLA and G. V. KELLER (Colorado School of Mines Press, Golden, CO), 127-151.

ALFANO, L. (1993): Geoelectrical methods applied to structures of arbitrary shapes, *J. Appl. Geophys.*, **29**, 181-192.

AL'PIN, L.M. (1950): The theory of dipole sounding, *Consultant Bureau*, **1966**, 1-10.

AL'PIN, L.M. (1958): Transformation of sounding curves, *Consultant Bureau*, **1966**, 61-114.

DIETER, K., N.R. PATERSON and F.S. GRANT (1969): IP and resistive type curves for three-dimensional bodies, *Geophysics*, **34**, 615-632.

OKABE, M. (1981): Boundary element method for the arbitrary inhomogeneous problem in electrical prospecting, *Geophys. Prospect.*, **29**, 39-59.

PATELLA, D. (1974): On the transformation of dipole to Schlumberger sounding curves, *Geophys. Prospect.*, **22**, 315-329.

YOUNG, D.M. (1971): *Iterative Solution of Large Linear Systems* (Associated Press, New York), pp. 570.